Title

REGGE-POLE MODEL FOR nN AND NN SECONDARY MAXIMA AND THE THE NO-COMPENSATION MECHANISM

Permalink

https://escholarship.org/uc/item/1050g8vc

Authors

Chiu, Charles B.
Chu, Shu-Yuan
Wang, Ling-Lie.

Publication Date

1967-01-17

UCRL-17339

University of California

Ernest O. Lawrence Radiation Laboratory

REGGE-POLE MODEL FOR πN AND NN SECONDARY MAXIMA AND THE NO-COMPENSATION MECHANISM

Berkeley, California

3 ω

Submitted to Physical Review Letters

UCRL-17339
Preprint

UNIVERSITY OF CALIFORNIA

Lawrence Radiation Laboratory
Berkeley, California

AEC Contract No. W-7405-eng-48

REGGE-POLE MODEL FOR πN AND NN SECONDARY MAXIMA AND THE NO-COMPENSATION MECHANISM

Charles B. Chiu, Shu-Yuan Chu, and Ling-Lie Wang

January 17, 1967

REGGE-POLE MODEL FOR πN AND NN SECONDARY MAXIMA AND THE NO-COMPENSATION MECHANISM*

Charles B. Chiu, Shu-Yuan Chu, and Ling-Lie Wang

Lawrence Radiation Laboratory
University of California
Berkeley, California

January 17, 1967

A pronounced dip-bump structure has been observed in both the π^+p and π^-p differential cross sections (dcs) as shown in Fig. 1. The similarity between the $\pi^\pm p$ secondary maxima and their smooth variation with energy indicates that they are dominated by the t-channel $(\pi\pi \rightarrow N\bar{N})$ exchange. Since the secondary maximum in $\pi^-p \rightarrow \pi^0 n$ is only 1/4 that in $\pi^\pm p$, the $\pi^\pm p$ bumps here must be dominated by the exchange of $I = 0$ state. We have checked that $(d\sigma/dt)$ $(I = 0)$ in the secondary bump region can be approximately fitted in a model-independent way by

$$\frac{d\sigma}{dt}(I = 0) = F(t)\, E_L^{2\alpha_{\text{eff}}-2} . \tag{1}$$

At $t = -1.4$ (GeV c)^2, near the peak of the secondary bump, the effective power, α_{eff}, corresponding to the rapid fall of the bump below 8 GeV/c is somewhere between -0.4 and -0.9. As usual, we assume the $I = 0$ t-channel exchange is dominated by the Regge trajectories P and P'. The slope of the P trajectory is small, as is suggested by the observed nonshrinking diffraction peak at high energies. Thus the negative value of α_{eff} in the secondary bump region is mainly associated with the P' trajectory. With a $t = 0$ intercept[2] above 0.5, the P' trajectory will have to pass through zero before the bump region.

Recently dips in the dcs have been associated with the vanishing of the contributions of some Regge trajectories.[3] Frautschi has suggested[4] that the dip in the elastic $\pi^{\pm}p$ dcs could be associated with the vanishing of the helicity-flip amplitude of P' at $\alpha_{P'} = 0$, a possibility allowed by the so-called Chew mechanism.[5] We investigated this situation extensively by fitting the secondary bump shown in Fig. 1, together with the high-energy data.[6] Our solutions, with reasonable fits to the secondary bump, do not have good χ^2 values for the high-energy data. However, a different possibility is that the helicity-nonflip amplitude of P' can vanish at $\alpha_{P'} = 0$, if the P' trajectory chooses what we call the "no-compensation mechanism".[7,8] The no-compensation mechanism for P' means that P' couples to the nonsense channel, and the residue of the nonsense-nonsense (nn) amplitude vanishes. Thus there is no pole in the nonsense-nonsense amplitude, and it is not necessary to have a compensating trajectory to cancel the pole as needed for the Gell-Mann mechanism. A detailed discussion of the α factors for these mechanisms is given in Ref. 7. Using this no-compensation mechanism, we obtain a better solution with much lower χ^2 value for the high-energy data. These two mechanisms also give different predictions to $\pi^{\pm}p$ polarizations. (We shall return to this point later.) In this letter, we discuss our results briefly and present in the figure captions some values of the parameters we used. The details will be presented elsewhere.[9]

We define

$$\frac{d\sigma}{dt} = \frac{1}{4\pi\, s\, p^2} \left(|f_{ss}|^2 + |\sin\theta_t|^2\, |f_{sn}|^2 \right), \qquad (2)$$

where p is the momentum in the s-channel c.m. system, θ_t is the scattering angle in the t-channel c.m. system, f_{ss} and f_{sn} are t-channel helicity nonflip (sense-sense) and flip (sense-nonsense) amplitudes respectively. The amplitudes f_{sn}^{P} and $f_{sn}^{P'}$ are constrained by the high-energy data to be small in the samll $|t|$ region. Using the no-compensation mechanism for both P and P' (the no-compensation mechanism is not crucial for P, since α_P is relatively flat, but for uniformity we use the same α factors in P as in P'), we fit the data both with and without these amplitudes, finding the χ^2 for these two cases to be essentially the same. We present here the solution with $f_{sn}^{P} = f_{sn}^{P'} = 0$. The ss amplitudes for P and P' are parameterized as follows:

$$f_{ss}^{P,P'} = (1 - \frac{t}{4M_N^2})^{-\frac{1}{2}} \alpha^2(\alpha + 1)^2 \xi C_0 \exp(C_1 t) (E_L)^{\alpha}, \qquad (3)$$

where ξ stands for the signature factor $-[\exp(-i\pi\alpha) \pm 1]/\sin\pi\alpha$. The ρ amplitudes we used are essentially the same as used in Ref. 6.

In our fit, the essential feature of the dip-bump structure is reproduced reasonably well as illustrated in Fig. 1. The fit to the high-energy data points for $|t| < 1$ is as good as that presented in Ref. 6. The dip in the $\pi^{\pm}p$ dcs of our solution is formed by the vanishing of $f_{ss}^{P'}$ at $\alpha_{P'} = 0$ $(t \approx -0.55)$ with a smooth and rapidly falling (in t) background f_{ss}^{P}. Since the magnitude of f_{ss}^{P} near $\alpha_{P'} = 0$ is substantial, the position of the dip has been shifted considerably from that of $\alpha_{P'} = 0$. Furthermore, it moves out slightly as the energy is increased, because f_{ss}^{P} decreases in magnitude slower than $f_{ss}^{P'}$. From Eq. (3) the contribution of P' vanishes at $\alpha_{P'} = -1$, so the bump structure requires some curvature in $\alpha_{P'}$. We use the form $\alpha_{P'} = \alpha_0 + \alpha_1 t + \alpha_2 t^2$. The slope of P is found to be between 0.3 and 0.4 $(\text{GeV}/c)^{-2}$. This nonzero slope of P compensates the antishrinkage effect[10] of the P' contribution to reproduce the observed nonshrinking forward peak of $\pi^{\pm}p$.

Now we discuss the different predictions for $\pi^{\pm}p$ polarizations in the dip region $t = -0.8$ to -1.0. In our solution for the Chew mechanism, the polarization is contributed mainly by the interference between f_{ss}^{P} and $f_{sn}^{P'}$. It predicts a large polarization with the same sign for $\pi^{+}p$ and $\pi^{-}p$. On the other hand, for the solution with the no-compensation mechanism, the interference between f_{ss}^{P}, $f_{ss}^{P'}$, and f_{sn}^{ρ} dominates, so the $\pi^{+}p$ and the $\pi^{-}p$ polarizations have opposite sign. The polarization data[11] around 2-3 GeV/c do have opposite signs for $\pi^{+}p$ and $\pi^{-}p$, but due to the uncertainty of the direct-channel resonance contribution, this evidence could not be regarded as conclusive. Confirmation of this opposite sign in this t region in future higher-energy experiments (say 6 to 10 GeV/c) will give additional support for this no-compensation mechanism.

The pp and the $\bar{p}p$ dcs are displayed in Fig. 2. We want to see whether the quite distinct features in the pp and the $\bar{p}p$ dcs can be fitted consistently by the no-compensation mechanism for P'. By usual arguments,[12] the ss amplitudes are dominated by P, P', and ω. The magnitude of sn and nn amplitudes for P and P' are expected to be small from the πN analysis through factorization. Although the sn and nn amplitudes will be needed to fit the polarization, we find that, in explaining the $\bar{p}p$ dip-bump structure and the pp relatively smooth behavior, inclusion of the nonsense amplitudes is not crucial. Since we try to explain only the gross features of the existing dcs data, for simplicity, we neglect all the sn and nn amplitudes.

Thus we define

$$\frac{d\sigma}{dt} = \frac{1}{4\pi\ s\ p^2} |f_{ss}|^2, \tag{4}$$

where

$$f_{ss}^{P,P'} = (1 - t/4M_N^2)^{-1}\ \alpha^2(\alpha + 1)^2\ \xi\ C_0\ \exp(C_1 t)\ (E_L)^{\alpha}, \tag{5}$$

$$f_{ss}^{\omega} = (1 - t/4M_N^2)^{-1}\ (1 - t/t_0)\ (\alpha + 1)\ \xi\ C_0\ \exp(C_1 t)\ (E_L)^{\alpha}\ . \tag{6}$$

As usual, the extra factor $(1 - t/t_0)$ in f_{ss}^{ω} is introduced to explain the change in sign of the difference of the pp and the $\bar{p}p$ dcs. The trajectories P and P' have already been determined in the πN analysis. The ω trajectory is parameterized as $\alpha_\omega = \alpha_0 + \alpha_1 t + \alpha_2 t^2$.

The pp and $\bar{p}p$ dcs data shown in Fig. 2 together with the total cross section data[13] are included in a least-square fit. In our solution, $f_{ss}^{P'}$ is small around the dip region because of its zero at $\alpha_{P'} = 0$. The dip-bump structure is mainly produced by the interference between f_{ss}^{P} and f_{ss}^{ω}. In the pp case, f_{ss}^{P} interferes with f_{ss}^{ω} with opposite sign and gives a smooth and dominating contribution. The zero in $f_{ss}^{P'}$ at $\alpha_{P'} = 0$ gives the slight curvature in the pp dcs in the large $|t|$ region. The fit to the total-cross-section data is adequate down to energies as low as 2.5 GeV/c. The Re/Im ratio of pp elastic scattering[14] from our solution is consistent with the available data above 10 GeV/c. This ratio is within two standard deviations of the allowed experimental value down to 2.5 GeV/c.[9]

To complement the present available dcs and pp polarization data,[15] we suggest an accurate measurement of the pp elastic dcs at 3 GeV/c from $t = -0.3$ to -1.0 be made, although it is very plausible, from the 5- and 7-GeV/c measurements in the same t region, that the behavior should be smooth. Perhaps more important is a more accurate and extensive measurement of the $\bar{p}p$ dcs in the t region from -0.4 to -1.0 and energy range from 2 to 8 GeV/c. We also suggest measurements of $\bar{p}p$ polarization in the similar region. Then, a more accurate analysis including all the nonsense amplitudes will be possible.

We thank Professor Geoffrey F. Chew for suggesting this study and for his advice throughout the development of this work. We are grateful to Professor Stanley Mandelstam for his interest in this work and invaluable discussions. We thank Dr. V. Barger, Dr. R. J. N. Phillips, and Dr. A. V. Stirling for helpful discussions on the numerical analysis.

FOOTNOTES AND REFERENCES

[*] This work was done under the auspices of the U. S. Atomic Energy Commission.

1. A. S. Carroll et al., Phys. Rev. Letters 16, 288 (1966); Saclay-Orsay Collaboration, Phys. Letters 20, 75 (1966).
2. J. Scanio, Lawrence Radiation Laboratory report UCRL-16766, 1966, (submitted to Phys. Rev., 1966). M. Restignoli et al., Phys. Rev. 150, 1389 (1966).
3. G. Höhler et al., Phys. Letters 20, 79 (1966); F. Arbab et al., Phys. Rev. 147, 1045 (1966). C. Chiu and J. Stack, Lawrence Radiation Laboratory report UCRL-16745, 1966 (to be published in Phys. Rev.). L. L. Wang, Phys. Rev. Letters 16, 756 (1966).
4. S. Frautschi, Phys. Rev. Letters 17, 722 (1966).
5. G. Chew, Phys. Rev. Letters 16, 60 (1966).
6. The high-energy data we used are essentially the same as those used in the paper by C. Chiu, R. Phillips, and W. Rarita, Lawrence Radiation Laboratory report UCRL-16940, 1966 (to be published in Phys. Rev.).
7. L. L. Wang, Lawrence Radiation Laboratory report UCRL-17053, 1966 (to be published in Phys. Rev.). This particular mechanism, which gives a zero at $\alpha_{P'} = 0$ in the helicity-nonflip amplitude, and the Chew mechanism are mentioned in footnote 14 of this reference.
8. We have studied the $N\overline{N}$ system in the potential theory of this no-compensation mechanism. We find that the residues do not

vanish at $\alpha = 0$, and thus the no-compensation mechanism cannot happen here. This is because $\alpha = 0$ is the first nonsense value in the $N\bar{N}$ system. However, from this study it is very plausible that this mechanism can happen in higher spin systems, where $\alpha = 0$ will be the second or third nonsense value. We thank Professor S. Mandelstam and Mr. Chung-I Tan for helpful discussions on this study.

9. C. Chiu, S. Y. Chu, and L. L. Wang, to be published.
10. Due to the zero in the $f_{ss}^{P'}$, the contribution of P' to the dcs is steeper than that of P. In addition, the contribution of P' falls off faster than that of P as energy increases. With these two factors, the P' contribution gives an antishrinkage effect.
11. O. Chamberlain et al., Phys. Rev. Letters 17, 975 (1966).
12. W. Rarita et al., Phys. Rev. Letters 12, 206 (1964).
13. W. Galbraith et al., Phys. Rev. 138, B913 (1965). D. Bugg et al., Phys. Rev. 146, 980 (1966).
14. See A. R. Clyde, Ph. D. thesis, University of California, Berkeley, 1966 (unpublished). See also the references therein.
15. P. Grannis et al., Lawrence Radiation Laboratory report UCRL-16750, 1966 (submitted to Phys. Rev. 1966).

FIGURE LEGENDS

Fig. 1. The $\pi^{\pm}p$ dcs. $\pi^{+}p$--o, ◬, ▽, □ at 2.5, 3, 3.5, and 4 GeV/c respecitvely by Coffin etal., Phys. Rev. Letters 17, 458 (1966); ◈ at 6.8 GeV/c by Foley et al., Phys. Rev. Letters 11, 425 (1963); ⊙ and ◇ at 8 and 12 GeV/c by Orear et al., Cornell-Michigan-BNL preprint submitted to Phys. Rev. July 1966. $\pi^{-}p$--o, ◬, □ at 2.5, 3, and 4 GeV/c by Coffin et al., Phys. Rev. Letters 15, 838 (1965); ◈ at 7 GeV/c by Foley et al., Phys. Rev. Letters 11, 425 (1963); ⊙ and ◇ at 8 and 12 GeV/c by Orear et al., Cornell-Michigan-BNL preprint July 1966. The solid curves are out fit using no-compensation mechanism with: $C_0 = 2.16$ mb $(\text{GeV}/c)^2$, $C_1 = 1.16$ $(\text{GeV}/c)^{-2}$ for P, $C_0 = 7.49$, $C_1 = -1.92$ for P' and $\alpha_P = 1.0 + 0.334\ t$, $\alpha_{P'} = 0.629 + 1.307\ t + 0.288\ t^2$.

Fig. 2. The pp and $\bar{p}p$ dcs. Data points: pp -- ▼, ⊙, ◬ at 3,5, and 7 GeV/c respecitvely, Ref. 14; ▽ at 3.04 GeV/c by Cork et al., Phys. Rev. 107, 859 (1957); ▨ at 19.6 GeV/c by Foley et al., Phys. Rev. Letters 11, 425 (1963). $\bar{p}p$--◬, □ at 2 and 2.5 GeV/c by Barish et al., Phys. Rev. Letters 17, 720 (1966); △ at 3 GeV/c by Escoubes et al., Physics Letters 5, 132 (1963);o at 4 GeV/c by Czyzewski et al., Physics Letters 15, 188 (1965); o at 12 GeV/c by Foley et al., Phys. Rev. Letters 15, 45 (1965). The solid curves are our fit with: $C_0 = 7.84$, $C_1 = 2.41$ for P, $C_0 = 27.9$, $C_1 = -1.39$ for P', $C_0 = 17.4$, $C_1 = 1.50$,

$t_0 = 0.147$ for ω, $\alpha_\omega = 0.414 + 0.986\,t + 0.265\,t^2$. Values of the fitted $\bar{p}p$ dcs by integrating over corresponding bin intervals: ▲ 3 GeV/c, × 4 GeV/c.

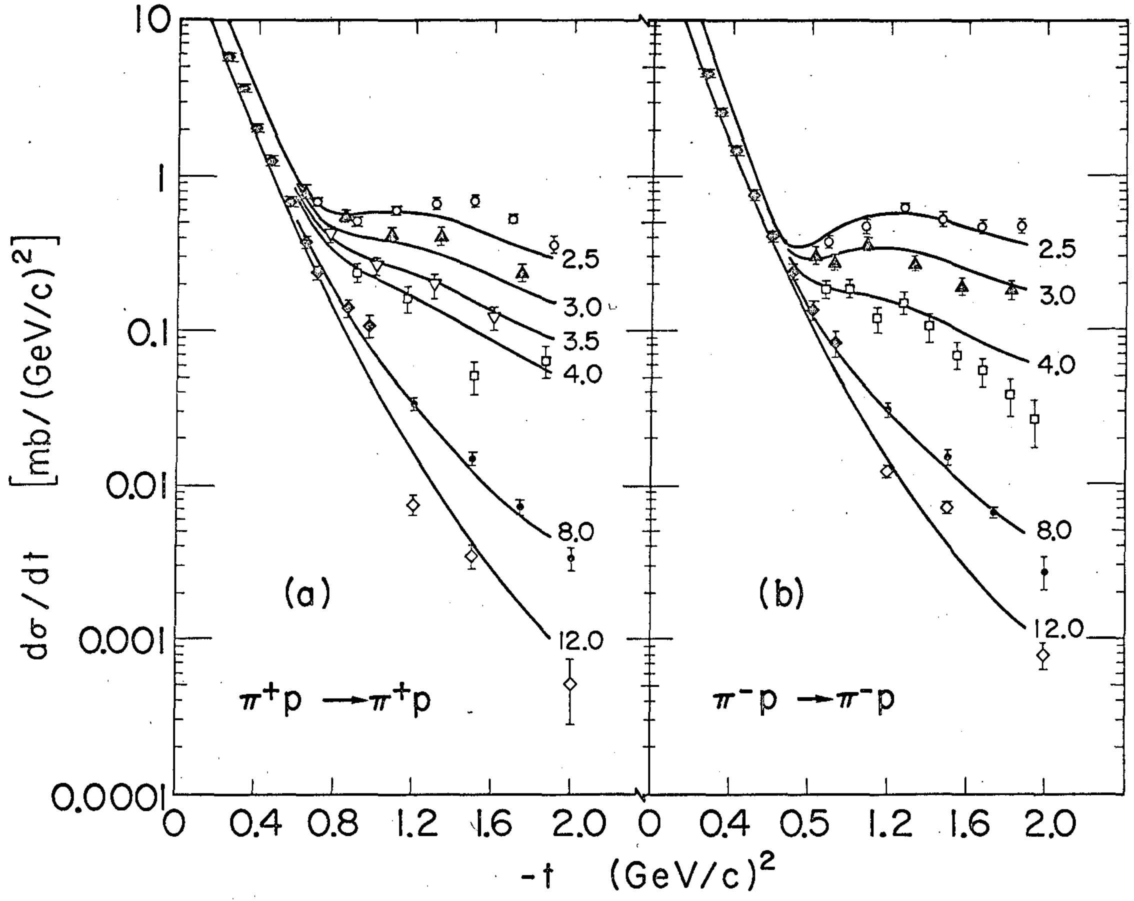

XBL671-328

Fig. 1

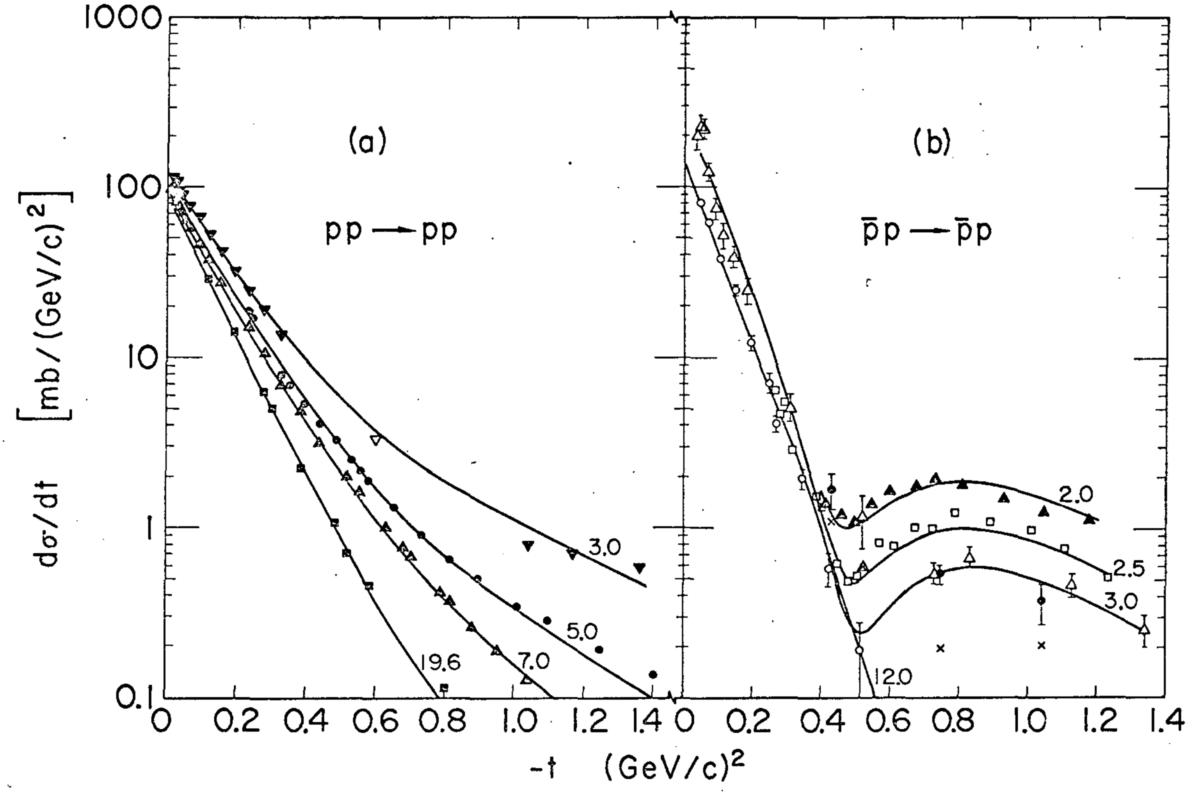

XBL671-329

Fig. 2